Circadian key component CLOCK/BMAL1 interferes with segmentation clock in mouse embryonic organoids

Authors: Yasuhiro Umemura[a], Nobuya Koike[a], Yoshiki Tsuchiya[a], Hitomi Watanabe[b], Gen Kondoh[b], Ryoichiro Kageyama[c], and Kazuhiro Yagita[a,*].

Affiliations:

[a]Department of Physiology and Systems Bioscience, Kyoto Prefectural University of Medicine, Kawaramachi-Hirokoji, Kyoto 602-8566, Japan.

[b]Laboratory of Integrative Biological Science, Institute for Frontier Life and Medical Sciences, Kyoto University, Kyoto 606-8501, Japan.

[c]Laboratory of Growth Regulation System, Institute for Frontier Life and Medical Sciences, Kyoto University, Kyoto 606-8507, Japan.

*Correspondence to: Kazuhiro Yagita

Email: kyagita@koto.kpu-m.ac.jp

Author Contributions: Y.U. and K.Y. designed the research; Y.U., Y.T., H.W., G.K., and K.Y. performed the research; Y.U., N.K., Y.T., R.K., and K.Y. analyzed the data; Y.U., N.K., and K.Y. wrote the paper

Competing Interest Statement: The authors declare no competing interests

Abstract

In mammals, circadian clocks are strictly suppressed during early embryonic stages as well as pluripotent stem cells, by the lack of CLOCK/BMAL1 mediated circadian feedback loops. During ontogenesis, the innate circadian clocks emerge gradually at a late developmental stage, then, with which the circadian temporal order is invested in each cell level throughout a body. Meanwhile, in the early developmental stage, a segmented body plan is essential for an intact developmental process and somitogenesis is controlled by another cell-autonomous oscillator, the segmentation clock, in the posterior presomitic mesoderm (PSM). In the present study, focusing upon the interaction between circadian key components and the segmentation clock, we investigated the effect of the CLOCK/BMAL1 on the segmentation clock *Hes7* oscillation, revealing that the expression of functional CLOCK/BMAL1 severely interferes with the ultradian rhythm of segmentation clock in induced PSM and gastruloids. RNA sequencing analysis showed that the premature expression of CLOCK/BMAL1 affects the *Hes7* transcription and its regulatory pathways. These results suggest that the suppression of CLOCK/BMAL1-mediated transcriptional regulation during the somitogenesis may be inevitable for intact mammalian development.

Introduction

The circadian clock is the cell-autonomous time-keeping system generating the orderly regulated various physiological functions, which enables cells, organs, and systems to adapt to the cyclic environment of the rotating Earth (1-5). The core architecture of the circadian molecular clock consists of negative transcriptional/translational feedback loops (TTFLs) composed of a set of circadian clock genes, including *Bmal1*, *Clock*, *Period* (*Per1*, *2*, *3*), and *Cryptochrome* (*Cry1*, *2*), functioning under the control of E-box elements (2, 6). The kernel of TTFLs is composed of heterodimerized CLOCK/BMAL1 key transcriptional factors that positively regulate the circadian output genes, as well as *Per* and *Cry* genes via E-box. PERs and CRYs inhibit CLOCK/BMAL1 transcriptional activity, and the negative feedback loops between these genes generate oscillations of approximately 24 hr.

In mammalian development, it has been demonstrated that early embryos and pluripotent stem cells have no apparent circadian molecular oscillations (7-11), whereas the innate circadian clock develops during ontogenesis and is established at a late developmental stage (12-15). Regarding the mechanisms regulating circadian clock development, using an *in vitro* model of embryonic stem cell (ESC) differentiation and mouse embryos, it was shown that prolonged posttranscriptional mechanisms, such as suppressed translation of CLOCK protein and

52 predominant cytoplasmic localization of PER proteins, inhibit the establishment of the circadian
53 TTFL cycle (16-18). Although it was revealed that the multiple mechanisms strictly suppress the
54 circadian molecular clock in the undifferentiated cells and early stage embryos, the biological and
55 physiological significance of the delayed emergence of circadian clock oscillation in mammalian
56 embryos has been unknown.

57 In the early developmental stages, a segmented body plan is essential for an intact
58 developmental process. Somitogenesis is related to another cell-autonomous oscillator, the
59 segmentation clock, in the posterior presomitic mesoderm (PSM) (19, 20). The mouse
60 segmentation clock is underlain by a negative feedback loop involving *Hes7* oscillation (21, 22).
61 HES7 is a key transcriptional factor that represses its own expression and oscillates through a
62 negative feedback loop in a period of 2–3 hr in mouse and 4–5 hr in humans. The NOTCH, WNT,
63 and fibroblast growth factor signaling pathways are involved in the regulation of the *Hes7*
64 oscillator and its intercellular synchronization (20). In mammals, two different types of rhythm
65 sequentially emerge during the developmental process, however, there is a lack of knowledge
66 about the biological significance of the rhythm conversion during development.

67 In this study, focusing on the relationship between circadian clock and segmentation clock,
68 we investigated the effect of the premature expression of CLOCK/BMAL1 on the segmentation
69 clock oscillation, and revealed severe interference with the ultradian rhythm of segmentation clock
70 in iPSM and gastruloids. RNA sequencing analysis showed that CLOCK/BMAL1 affects the *Hes7*
71 transcription and its regulatory pathways. These findings highlight that the suppression of
72 functional CLOCK/BMAL1, which leads to arrest the circadian clock oscillation, during the early
73 to mid-developmental stage may be inevitable for the intact process of mammalian embryogenesis.

74

75

76

77 **Results**

78 **A circadian clock gene, *Per1*, and a segmentation clock gene, *Hes7*, are adjacent genes in the**
79 **mammalian genome**

80 In mammals, the temporal relationship between the segmentation clock and circadian clock
81 appears to be mutually exclusive (**Fig. S1**) (12-15, 19, 20). To explore the functional interaction
82 between these two biological rhythms with different frequencies during the developmental process,

83 we focused on the genomic architecture of genes comprising circadian and segmentation clocks,
84 respectively. Intriguingly, one of the core circadian clock genes, *Per1*, is physically adjacent to an
85 essential component of the segmentation clock, *Hes7*, in a genomic region conserved in higher
86 vertebrates, including mice and humans. The *Per1* homolog *Per2* is adjacent to the *Hes7* homolog
87 *Hes6* in the genome (**Fig. 1A**). Since *Hes7* exhibits the essential characteristics of a segmentation
88 clock (23) and neighboring genes can influence the expressions with each other during
89 somitogenesis in zebrafish (24), we focused on the effect of the regulation mechanism of the
90 circadian clock on segmentation clock oscillation. Therefore, we investigated the effect of the
91 CLOCK/BMAL1-mediated activation of *Per1* transcription on the segmentation clock oscillation
92 in induced presomitic mesoderm (iPSM), an *in vitro* recapitulating model of a segmentation clock,
93 using ESCs carrying the *Hes7*-promoter-driven luciferase reporter (*pHes7-luc*) (25) (**Fig. 1B**). In
94 the iPSM, the pluripotent markers have not yet been down-regulated sufficiently as previously
95 reported (25), and the iPSM differentiated from $Per2^{Luc}$ ESCs showed no apparent circadian clock
96 oscillation (**Fig. S2A and B**). In addition, the immunostaining pattern of CLOCK, BMAL1, and
97 PER1 in the iPSMs was quite similar to that in the undifferentiated ESCs (**Fig. S2C**) (16, 17),
98 confirming that the circadian TTFL was not established and circadian clock oscillation was also
99 strictly suppressed in the iPSM by the common inhibitory molecular mechanisms to the
100 undifferentiated ESCs.

101 Because CLOCK/BMAL1 is key transcription regulator of circadian TTFL, and the
102 expression of CLOCK protein is suppressed post-transcriptionally in iPSM as well as ESCs and
103 early embryos (17), we established two ESC lines carrying both the doxycycline (dox)-inducible
104 *Clock* and *Bmal1* genes (**Fig. 1C**, **Fig. S3**). In iPSM differentiated from ESCs, the expression of
105 both *Clock/Bmal1* mRNA and CLOCK/BMAL1 proteins was confirmed after the addition of dox
106 (**Fig. 1 D and E**), and we found that overexpression of both *Clock* and *Bmal1* successfully
107 activated the expression of core clock genes (**Fig. 2A**). As the dominant negative mutant of *Bmal1*
108 (*Bmal1DN*) (26) co-expressed with *Clock* did not activate the *Per1/2* and *Cry1/2* genes, we
109 concluded that CLOCK/BMAL1 specifically activated the expression of these clock genes via an
110 E-box (**Fig. 1 C–E, 2A**). We then examined the expression of genes in *Hes7*, which is proximal to
111 *Per1*, and *Hes6*, which is proximal to *Per2* in the genome. The expression of *Clock/Bmal1* induced
112 by dox in the iPSM induced significant upregulation of the expression of the *Hes7*, but not *Hes6*,
113 gene (**Fig. 2B**). Similarly, we also observed the upregulation of *Hes7* expression by *Clock/Bmal1*
114 induction in the undifferentiated ESCs (**Fig. S4 A and B**). These results indicate that the circadian
115 components CLOCK/BMAL1 also affect the segmentation clock gene *Hes7*, as well as *Per1*.

116

117 **Inhibition of *Hes7* ultradian rhythm by CLOCK/BMAL1 in iPSM**

118 We next performed a functional analysis using the *in vitro* recapitulation model of a
119 segmentation clock oscillation in iPSM (25). The oscillations in bioluminescence from *pHes7-luc*
120 reporters were observed using a photomultiplier tube device (PMT) and an EM-CCD camera (**Fig.**
121 **3A**). We confirmed an oscillation of *Hes7*-promoter-driven bioluminescence with a period of
122 approximately 2.5–3 hr in control iPSM with or without dox using PMT and the EM-CCD camera
123 (**Fig. 3 B and C**). Traveling waves of *pHes7-luc* bioluminescence were observed, indicating that
124 the segmentation clock oscillation in iPSM was successfully recapitulated, consistent with a
125 previous report (25). Using this iPSM-based segmentation clock system, we investigated the effect
126 of *Clock/Bmal1* expression on *Hes7*-promoter-driven oscillation. The expression of *Clock/Bmal1*
127 genes (Dox+) resulted in defects of the oscillation in *Hes7* promoter activity, whereas *pHes7-luc*
128 bioluminescence continued to oscillate under Dox– conditions. Oscillation of the segmentation
129 clock was observed even during the induction of *Clock/Bmal1DN* (**Fig. 3D**), indicating that the
130 CLOCK/BMAL1-mediated mechanism interfered with the transcriptional oscillation of *Hes7*. A
131 traveling wave of *Hes7* promoter activity disappeared with the expression of *Clock/Bmal1* (**Fig. 3**
132 **E and F**), and dox-dependent arrest of *pHes7-luc* traveling wave (**Fig. 3 G and H**) clearly
133 demonstrated the CLOCK/BMAL1-mediated interference with *Hes7*-driven segmentation clock
134 oscillation in iPSM.

135

136 **Interference with somitogenesis-like segmentation by induction of CLOCK/BMAL1 in**
137 **gastruloids**

138 In addition, to explore the effect of CLOCK/BMAL1 expression on somitogenesis, we
139 established the ESC-derived embryonic organoids, gastruloids, recapitulating an embryo-like
140 organization, including somitogenesis-like process *in vitro* (27) (**Fig. 4A**). The *pHes7-luc*
141 bioluminescence represented a traveling wave accompanied by the formation of segment-like
142 structures with anteroposterior polarity, in which the gastruloids were stained with stripes of a
143 somite marker, *Uncx4.1*, by *in situ* hybridization (**Fig. 4 B–D**). Only dox treatment in control
144 gastruloids induced no change in the *pHes7-luc* bioluminescence oscillation and somitogenesis-
145 like process (**Fig. 4 E–G**). The dox-inducible *Clock/Bmal1* ESC line carrying *pHes7-luc* was
146 differentiated *in vitro* into gastruloids and produced the somitogenesis-like process without dox
147 (**Fig. 4 H–J**). In contrast, the dox-dependent induction of *Clock/Bmal1* expression in the
148 gastruloids interrupted the *pHes7-luc* oscillation and disrupted the somitogenesis-like structures
149 (**Fig. 4 K–M**). In gastruloids, the expression of both *Clock/Bmal1* mRNA was confirmed after the

addition of dox (**Fig. S5**). These results suggest that the premature expression of the circadian key transcriptional regulator CLOCK/BMAL1 critically interferes with not only *Hes7* oscillation, but also somitogenesis.

CLOCK/BMAL1-mediated interference in *Hes7* regulatory network

Next, to examine the perturbation mechanisms of the segmentation clock oscillation by the circadian components CLOCK/BMAL1, we analyzed the RNA sequencing (RNA-seq) data obtained from the total RNA of iPSM colonies. We extracted 509 upregulated and 88 downregulated differentially expressed genes (DEGs) after the induction of *Clock/Bma11* gene expression in iPSM colonies (**Fig. 5A**). A KEGG pathway enrichment analysis for the DEGs revealed enrichment of the WNT, MAPK, and NOTCH signaling pathways related to *Hes7* oscillation (28) (**Fig. 5B**). Almost all other ranked pathways also included the WNT, MAPK, and NOTCH signaling pathway-related genes (**Fig. 5B**). Similarly, enrichment of the WNT, MAPK, and NOTCH signaling pathways by *Clock/Bmal1* induction was also observed in the undifferentiated ESCs (**Fig. S6 A and B**). These findings indicate that the expression of CLOCK/BMAL1 affects the *Hes7*-related signaling pathways, which interferes with the feedback loop regulating *Hes7* oscillation. Intriguingly, in addition to *Hes7* gene expression, the expressions of *Aloxe3* in iPSM and *Aloxe3* and *Vamp2* in ESCs, the other contiguous genes with *Per1*, were upregulated with the induction of *Clock/Bmal1* expression, and this result was confirmed by quantitative RT-PCR (qPCR) (**Fig. 5 C–E**, **Fig. S6 C–E**) suggesting that forced expression of CLOCK/BMAL1 also affects a wide region around the *Hes7* gene locus on the same chromosome. These results suggest that the premature expression of the circadian components CLOCK/BMAL1 interfered with *Hes7* oscillation and somitogenesis by perturbing the *Hes7* expressions through indirect regulatory pathways (**Fig. 5F**). Because the loss of the *Hes7* ultradian expression rhythm in the mouse cause segmentation defects (22, 29), the oscillatory expression of *Hes7* is essential for mammalian development. Therefore, the results in this study suggest that it may be imperative that CLOCK/BMAL1 function is suppressed until the completion of segmentation and other related developmental events.

Discussion

180 Our present study showed that premature expression of circadian key components
181 CLOCK/BMAL1 severely interferes with the ultradian rhythm of the segmentation clock in iPSM
182 and gastruloids.

183 We have previously reported that during the early to mid-developmental stage, there are
184 multiple molecular mechanisms that underlie the strict suppression of circadian TTFLs, such as
185 the post-transcriptional suppression of CLOCK protein (17, 18) and the exclusive cytoplasmic
186 localization of PER proteins (16). Furthermore, we have also reported that the maternal circadian
187 clock cannot entrain the fetus until the establishment of the fetal circadian clock itself (17). These
188 results suggest that the circadian rhythm in mammalian embryos is rigorously suppressed by the
189 multilayered inhibitory mechanisms during the early to mid-developmental stage. During the
190 multilayered suppression of circadian clock oscillation, the ultradian temporal oscillation of *Hes7*
191 expression, segmentation clock, proceeds and forms the spatial repetitive structure of somites.

192 In the present study, we investigated the effect of the CLOCK/BMAL1-mediated activation
193 of *Per1* transcription on the segmentation clock oscillation by using the iPSM differentiated from
194 ESCs. It was suggested that, similar to the undifferentiated ESCs, circadian clock oscillation is
195 suppressed in the iPSM by the common mechanisms to the ESCs and early embryos (**see Fig. S2**).
196 Recently, it was reported that hundreds of genes including *Per1* also oscillates in the same phase
197 as *Hes7* ultradian rhythm in *in vitro*-PSM of both mouse and humans (30), suggesting that *Per1* is
198 deviated and free from the circadian gene regulatory mechanism of TTFL. These findings are
199 consistent with the previously reported observations indicating that the multilayered inhibitory
200 mechanisms including post-transcriptional inhibition of CLOCK and the predominant cytoplasmic
201 accumulation of PER1 do not allow the oscillation of circadian TTFL (17, 18). Interestingly,
202 although the expression of BMAL1 protein was observed even in ESCs (17), the dox-induced
203 CLOCK sole expression in ESCs resulted in the only partial upregulation of E-box driven circadian
204 clock genes (**Fig. S3**), raising the possibility that the endogenously expressed BMAL1 might be
205 post-translationally modified to not function. Therefore, in this study, we used ESC lines carrying
206 both the dox-inducible *Clock* and *Bmal1* genes as a model system of premature expression of
207 CLOCK/BMAL1 (**see Fig. 1C**).

208 We demonstrated that the expression of CLOCK/BMAL1 affected the WNT, MAPK, and
209 NOTCH signaling pathways related to *Hes7* oscillation in iPSM (**see Fig. 5 A and B**). In addition,
210 the premature expression of CLOCK/BMAL1 resulted in not only the up-regulation of *Per1*
211 expression but also the expressions of *Hes7*, *Aloxe3*, and *Vamp2*, localized adjacently on the *Per1*
212 genomic locus (**see Fig. 2 A and B, Fig. 5 C–E, Fig. S6 C–E**). In the iPSM, the up-regulation of
213 these gene expressions has already been induced after the 2-hour dox treatment (**see Fig. 2 A and**

214 **B, Fig. 5 C–E**). Considering that the *Per1* promoter harbors E-box elements with which
215 CLOCK/BMAL1 heterodimer has a much higher affinity than the other genomic region (31), the
216 immediate up-regulation of genes near *Per1* gene locus after the induction of CLOCK/BMAL1
217 expressions could be caused by the ripple effect (32). On the other hand, the bioluminescence from
218 *Hes7*-promoter driven luciferase reporters in the iPSMs not only lost cycling but also decreased
219 signal intensity in approximately 2 hours after the dox addition (**see Fig. 3D**), indicating that the
220 expression of CLOCK/BMAL1 in the iPSM has also inhibitory effects on the *Hes7* gene
221 expressions. Among components involved in the *Hes7*-regulatory signaling pathways, expression
222 of CLOCK/BMAL1 induced some negative regulators, such as the *Dusp* phosphatase family (33)
223 in the MAPK signaling pathway, *Sfrp* in the WNT signaling pathway (34), and *Lfng* in the NOTCH
224 signaling pathway (35) (**see Fig. 5B**). Therefore, the premature expression of CLOCK/BMAL1
225 first may upregulate *Hes7* transcription and induce subsequent downregulation of *Hes7* gene
226 expression by the induction of the negative regulators in addition to the HES7 autoinhibition.
227 Consequently, the premature expression of the circadian components CLOCK/BMAL1 interfered
228 with *Hes7* oscillation by perturbing the *Hes7* expression through various pathways.

229 In this study, we used a mouse embryonic organoid, gastruloids, as an *in vitro* recapitulation
230 model of somitogenesis-like process (27). The premature expression of CLOCK/BMAL1 in the
231 gastruloids disrupted not only the *Hes7* oscillation but also the striped structure of the somite
232 marker, *Uncx4.1* (**see Fig. 4M**). Because the RNA-seq analysis data showed that hundreds of genes
233 were affected by the induction of CLOCK/BMAL1 (**see Fig. 5A**), the possibility cannot be denied
234 that the premature expression of CLOCK/BMAL1 affects cell fates or characters. However, the
235 posterior structure in the gastruloids was held even after the induction of CLOCK/BMAL1 and
236 then continued to extend, concomitant with the decrease of *Hes7* bioluminescence signals and the
237 arrest of the *Hes7* oscillation (**see Fig. 4K**), suggesting that the premature expression of
238 CLOCK/BMAL1 interfered with the somitogenesis process by perturbing *Hes7* oscillation of the
239 segmentation clock.

240 In vitro recapitulation of embryonic process using iPSM and gastruloids has differences
241 such as no brain tissues comparing with in vivo process. However, key regulators of somitogenesis
242 we focus on in this study are expressed similarly between embryos and gastruloids using single-
243 cell RNA sequencing and spatial transcriptomics (27), and the in vitro recapitulation model enables
244 to analyze the *Hes7* oscillation in more detail using real-time imaging without maternal effects.

245 Our findings shown in this study indicated that the CLOCK/BMAL1, key components
246 regulating the circadian TTFL, affected and interfered with the segmentation clock. Considering
247 that transcriptional activation of CLOCK/BMAL1 is essential for the circadian regulatory

248 networks, these results suggest that the strict suppression of circadian molecular oscillatory
249 mechanisms during the early stage embryos is inevitable for the intact developmental process in
250 mammals. Therefore, this may be the biological and physiological significance of the delayed
251 emergence of circadian clock oscillation and the rhythm conversion observed in mammalian
252 development.

253

254

255 **Materials and Methods**

256 **Cell culture**

257 KY1.1 ESCs (7), referred to as ESC in the text, and *Per2*^{Luc} ESCs (5, 36) were maintained as
258 described previously (17). E14TG2a ESCs carrying *Hes7*-promoter-driven luciferase reporters
259 (25), referred to as *pHes7-luc* ESCs in the text, were maintained without feeder cells in DMEM
260 (Nacalai) supplemented with 15% fetal bovine serum (Hyclone), 2 mM L-glutamine (Nacalai), 1
261 mM nonessential amino acids (Nacalai), 100 μM StemSure® 2-mercaptoethanol solution (Wako),
262 1 mM sodium pyruvate (Nacalai), 100 units/mL penicillin and streptomycin (Nacalai), 1000
263 units/mL leukemia inhibitory factor (Wako), 3 μM CHIRON99021 (Wako or Tocris Biosciences),
264 and 1 μM PD0325901 (Wako) with 5% CO_2 at 37°C.

265

266 **Transfection and establishment of cell lines**

267 ESCs stably expressing dox-inducible *Clock/Bmal1* or *Clock/Bmal1DN* (I584X) were
268 established as described previously (17). For *TetO-Clock/Bmal1* or *TetO-Clock/Bmal1DN* ESCs,
269 KY1.1 ESCs or *pHes7-luc* ESCs were transfected using 10.5 μl of FuGENE 6 mixed with 1 μg of
270 pCAG-PBase, 1 μg of PB-TET-Clock (17), 1 μg of PB-TET-Bmal1 or PB-TET-Bmal1DN
271 (I584X), 1 μg of PB-CAG-rtTA Adv, and 0.5 μg of puromycin selection vector. The transfected
272 cells were grown in a culture medium supplemented with 2 μg/mL puromycin for two days. The
273 ESC colonies were picked and checked by qPCR after treatment with 500 ng/mL dox. For PB-
274 TET-Bmal1 and PB-TET-Bmal1DN (I584X), Bmal1 cDNA and Bmal1DN (I584X) cDNA (26)
275 were cloned into a PB-TET vector (37). For the *TetO-Clock Per2*^{Luc} ESCs, *Per2*^{Luc} ESCs were
276 established as described previously (17).

277

278 **Bioluminescence imaging**

279 The iPSM colonies were differentiated from the *pHes7-luc* ESCs and *Per2*^{Luc} ESCs as
280 described previously (25). The *Per2*^{Luc} ESCs were cultured without feeder cells in the ES medium
281 containing 3 μM CHIRON99021 and 1 μM PD0325901 before in vitro differentiation.
282 Bioluminescence imaging of single *pHes7-luc* iPSM colonies and *Per2*^{Luc} iPSM colonies was
283 performed in gelatin-coated 24-well black plates or 35-mm dishes (26). DMEM was used that was
284 supplemented with 15% Knock-out Serum Replacement (KSR), 2 mM L-glutamine, 1 mM
285 nonessential amino acids, 1 mM sodium pyruvate, 100 units/mL penicillin and streptomycin, 0.5%
286 DMSO, 1 μM CHIRON99021, and 0.1 μM LDN193189 (Sigma) containing 1 mM luciferin and
287 10 mM HEPES. For live imaging of single iPSM colonies using an EM-CCD camera, each iPSM
288 colony was cultured on a fibronectin-coated glass base dish for 6 h, and images were acquired
289 every 5 min with an exposure time of 10 sec (control) or 2.5 sec (*Clock/Bmal1* induction) under
290 5% CO_2 using an LV200 Bioluminescence Imaging System (Olympus).

291 Gastruloids were generated as described in a previous report (27). In total, 200–250 live
292 cells were plated in 40 μl of N2B27 medium into each well of a U-bottomed nontissue culture-
293 treated 96-well plate (Greinier 650185). After a 96-hr cultivation, the gastruloids were embedded
294 in 10% Matrigel (Corning 356231) containing 1 mM luciferin. For live imaging of single
295 gastruloids, the images were acquired every 5 min with an exposure time of 3.5 sec (*Clock/Bmal1*
296 induction) or 10 sec (control) under 5% CO_2 using the LV200 system. The Videos were analyzed
297 using the ImageJ software (38). Kymographs of the averaged bioluminescence intensity along the
298 straight or segmented line of 5-pixel width were generated using the plug-in KymoResliceWide.

299

300 ***In situ* hybridization**

301 Hybridization chain reaction (HCR) v3 was performed as described previously (27, 39) using
302 reagents procured from Molecular Instruments. *Uncx4.1* HCR probe (Accession NM_013702.3,
303 hairpin B1) was labeled with Alexa Fluor 488.

304

305 **Quantitative RT-PCR**

306 The iPSM colonies, ESCs, and gastruloids were washed with ice-cold PBS, and total RNA
307 was extracted using Isogen reagent (Nippon Gene) or miRNeasy Mini Kits (QIAGEN) according
308 to the manufacturer's instructions. To remove the feeder cells from ESCs cultured on a feeder

309 layer, the cells were treated with trypsin, and then the mixed cell populations were seeded on
310 gelatin-coated dishes and incubated for 25 min at 37°C three times in ES cell medium. Non-
311 attached ESCs were seeded in a gelatin-coated dish overnight and then treated with or without 500
312 ng/mL doxycycline for 6 hr. The iPSM colonies and gastruloids were treated with or without 1000
313 ng/mL doxycycline for 2 hr. First-strand cDNAs were synthesized with 1000 or 280 ng of total
314 RNA using M-MLV reverse transcriptase (Invitrogen) according to the manufacturer's
315 instructions. Quantitative PCR analysis was performed using the StepOnePlus™ Real-Time PCR
316 system (Applied Biosystems) and iTaq™ Universal SYBR Green Supermix (Bio-Rad
317 Laboratories). Standard PCR amplification protocols were applied, followed by dissociation-curve
318 analysis to confirm specificity. Transcription levels were normalized to the level of β-actin. The
319 following primer sequences were used:

320	*Bmal1*	Forward (F)	CCACCTCAGAGCCATTGATACA
321	*Bmal1*	Reverse (R)	GAGCAGGTTTAGTTCCACTTTGTCT
322	*Clock*	F	ATTTCAGCGTTCCCATTTGA
323	*Clock*	R	TGCCAACAAATTTACCTCCAG
324	*Per1*	F	CCCAGCTTTACCTGCAGAAG
325	*Per1*	R	ATGGTCGAAAGGAAGCCTCT
326	*Per2*	F	CAGCACGCTGGCAACCTTGAAGTAT
327	*Per2*	R	CAGGGCTGGCTCTCACTGGACATTA
328	*Cry1*	F	TGAGGCAAGCAGACTGAATATTG
329	*Cry1*	R	CCTCTGTACCGGGAAAGCTG
330	*Cry2*	F	CTGGCGAGAAGGTAGAGTGG
331	*Cry2*	R	GACGCAGAATTAGCCTTTGC
332	*Dbp*	F	CGAAGAACGTCATGATGCAG
333	*Dbp*	R	GGTTCCCCAACATGCTAAGA
334	*Hes6*	F	CAACGAGAGTCTTCAGGAGCTGCG
335	*Hes6*	R	GCATGCACTGGATGTAGCCAGCAG

Hes7	F	GAGAGGACCAGGGACCAGA
Hes7	R	TTCGCTCCCTCAAGTAGCC
Vamp2	F	GAGCTGGATGACCGTGCAGATG
Vamp2	R	ATGGCGCAGATCACTCCCAAGA
Aloxe3	F	AAGCCCGCCAAGAATGTTATC
Aloxe3	R	CGGTTCCCAGAGTTGTCATCC
Actb	F	GGCTGTATTCCCCTCCATCG
Actb	R	CCAGTTGGTAACAATGCCATGT

RNA-seq

The iPSM colonies and ESCs were washed with ice-cold PBS, and total RNA was extracted using miRNeasy Mini Kits (QIAGEN) according to the manufacturer's instructions. Total RNA sequencing was conducted by Macrogen Japan on an Illumina NovaSeq 6000 with 101-bp paired-end reads. After trimming the adaptor sequences using Trimmomatic (40), the reads that mapped to ribosomal DNA (GenBank: BK000964.1) (41) were filtered out and the sequence reads were mapped to the mouse genome (GRCm38/mm10) using STAR (42), as described previously (16). To obtain reliable alignments, reads with a mapping quality of less than ten were removed using SAM tools (43). The known canonical genes from GENCODE VM23 (44) were used for annotation, and the reads mapped to the gene bodies were quantified using Homer (45). The longest transcript for each gene was used for gene-level analysis. We assumed that a gene was expressed when there were more than 20 reads mapped on average to the gene body. Differential gene expression in the RNA-seq data was determined using DESeq2 with thresholds of FDR < 0.05, fold change > 1.5, and expression level cutoff > 0.1 FPKM (46). WebGestalt was used for KEGG pathway enrichment analysis (47). In the RNA-seq data using iPSM colonies, the reads mapped in the promoter (chr11:69115096-69120473) and 3′ UTR (chr11:69122995-69123324) of *Hes7* were filtered out to eliminate transcripts from the *pHes7-luc* reporter transgene. The heatmaps of gene expression and KEGG pathways were generated with R using the pheatmap and pathview packages, respectively.

365 **Immunostaining**

366 The iPSM colonies were fixed in cold methanol for 15 min at room temperature. The fixed
367 iPSM was blocked with 1% BSA or 5% skim milk overnight at 4°C and then incubated with anti-
368 CLOCK mouse antibody (CLSP4) (48), anti-BMAL1 mouse antibody (MBL, JAPAN), anti-
369 BMAL1 guinea pig antibody (16), or anti-PER1 rabbit antibody (AB2201, Millipore) overnight at
370 4°C. After washing in 1% BSA, the iPSM colonies were incubated with a CF™488A-conjugated
371 donkey anti-mouse IgG (Nacalai), Cy3-conjugated goat anti-guinea pig IgG (Jackson),
372 DyLight™488-conjugated donkey anti-rabbit IgG (Jackson) for 2 hr at 4°C, and the nuclei were
373 stained with TO-PRO®-3 1:1000 (Thermo Fisher Scientific, USA) for 10–20 min. The iPSM
374 colonies were washed in 1% BSA and observed using an LSM510 or 900 confocal laser scanning
375 microscope (Zeiss).

376

377 **Data availability**

378 RNA sequence data are available at the Gene Expression Omnibus. All other datasets generated in
379 this study are available from the corresponding author upon reasonable request.

380

381

382 **Acknowledgments:** We thank the Yagita lab members for technical assistance. This work was
383 supported in part by grants-in-aid for scientific research from the Japan Society for the Promotion
384 of Science to Y.U. (19K06679) and K.Y. (18H02600), the Cooperative Research Program (Joint
385 Usage/Research Center program) of the Institute for Frontier Life and Medical Sciences, Kyoto
386 University (K.Y. and G.K.)

387

388 **References**

389 1. A. Balsalobre, F. Damiola, U. Schibler, A serum shock induces circadian gene expression
390 in mammalian tissue culture cells. *Cell* **93**, 929-937 (1998).

391 2. J. S. Takahashi, Transcriptional architecture of the mammalian circadian clock. *Nat Rev*
392 *Genet* **18**, 164-179 (2017).

393 3. K. Yagita, F. Tamanini, G. T. van Der Horst, H. Okamura, Molecular mechanisms of the
394 biological clock in cultured fibroblasts. *Science* **292**, 278-281 (2001).

395 4. S. Yamazaki *et al.*, Resetting central and peripheral circadian oscillators in transgenic rats.
396 *Science* **288**, 682-685 (2000).

397 5. S. H. Yoo *et al.*, PERIOD2::LUCIFERASE real-time reporting of circadian dynamics
398 reveals persistent circadian oscillations in mouse peripheral tissues. *Proc Natl Acad Sci U*
399 *S A* **101**, 5339-5346 (2004).

400 6. J. B. Hogenesch, H. R. Ueda, Understanding systems-level properties: timely stories from
401 the study of clocks. *Nat Rev Genet* **12**, 407-416 (2011).

402 7. K. Yagita *et al.*, Development of the circadian oscillator during differentiation of mouse
403 embryonic stem cells in vitro. *Proc Natl Acad Sci U S A* **107**, 3846-3851 (2010).

404 8. J. D. Alvarez, D. Chen, E. Storer, A. Sehgal, Non-cyclic and developmental stage-specific
405 expression of circadian clock proteins during murine spermatogenesis. *Biol Reprod* **69**, 81-
406 91 (2003).

407 9. T. Amano *et al.*, Expression and functional analyses of circadian genes in mouse oocytes
408 and preimplantation embryos: Cry1 is involved in the meiotic process independently of
409 circadian clock regulation. *Biol Reprod* **80**, 473-483 (2009).

410 10. E. Kowalska, E. Moriggi, C. Bauer, C. Dibner, S. A. Brown, The circadian clock starts
411 ticking at a developmentally early stage. *J Biol Rhythms* **25**, 442-449 (2010).

412 11. D. Morse, N. Cermakian, S. Brancorsini, M. Parvinen, P. Sassone-Corsi, No circadian
413 rhythms in testis: Period1 expression is clock independent and developmentally regulated
414 in the mouse. *Mol Endocrinol* **17**, 141-151 (2003).

415 12. F. C. Davis, R. A. Gorski, Development of hamster circadian rhythms: role of the maternal
416 suprachiasmatic nucleus. *J Comp Physiol A* **162**, 601-610 (1988).

417 13. C. Jud, U. Albrecht, Circadian rhythms in murine pups develop in absence of a functional
418 maternal circadian clock. *J Biol Rhythms* **21**, 149-154 (2006).

419 14. S. M. Reppert, W. J. Schwartz, Maternal suprachiasmatic nuclei are necessary for maternal
420 coordination of the developing circadian system. *J Neurosci* **6**, 2724-2729 (1986).

421 15. V. Carmona-Alcocer *et al.*, Ontogeny of Circadian Rhythms and Synchrony in the
422 Suprachiasmatic Nucleus. *J Neurosci* **38**, 1326-1334 (2018).

423 16. Y. Umemura *et al.*, Transcriptional program of Kpna2/Importin-alpha2 regulates cellular
424 differentiation-coupled circadian clock development in mammalian cells. *Proc Natl Acad*
425 *Sci U S A* **111**, E5039-5048 (2014).

426 17. Y. Umemura *et al.*, Involvement of posttranscriptional regulation of Clock in the
427 emergence of circadian clock oscillation during mouse development. *Proc Natl Acad Sci*
428 *U S A* **114**, E7479-E7488 (2017).

429 18. Y. Umemura, I. Maki, Y. Tsuchiya, N. Koike, K. Yagita, Human Circadian Molecular
430 Oscillation Development Using Induced Pluripotent Stem Cells. *J Biol Rhythms*
431 10.1177/0748730419865436, 748730419865436 (2019).

432 19. Y. Harima, I. Imayoshi, H. Shimojo, T. Kobayashi, R. Kageyama, The roles and
433 mechanism of ultradian oscillatory expression of the mouse Hes genes. *Semin Cell Dev*
434 *Biol* **34**, 85-90 (2014).

435 20. A. Hubaud, O. Pourquie, Signalling dynamics in vertebrate segmentation. *Nat Rev Mol*
436 *Cell Biol* **15**, 709-721 (2014).

437 21. Y. Bessho, H. Hirata, Y. Masamizu, R. Kageyama, Periodic repression by the bHLH factor
438 Hes7 is an essential mechanism for the somite segmentation clock. *Genes Dev* **17**, 1451-
439 1456 (2003).

440 22. Y. Takashima, T. Ohtsuka, A. Gonzalez, H. Miyachi, R. Kageyama, Intronic delay is
441 essential for oscillatory expression in the segmentation clock. *Proc Natl Acad Sci U S A*
442 **108**, 3300-3305 (2011).

443 23. Y. Bessho *et al.*, Dynamic expression and essential functions of Hes7 in somite
444 segmentation. *Genes Dev* **15**, 2642-2647 (2001).

445 24. O. Q. H. Zinani, K. Keseroglu, A. Ay, E. M. Ozbudak, Pairing of segmentation clock genes
446 drives robust pattern formation. *Nature* **589**, 431-436 (2021).

447 25. M. Matsumiya, T. Tomita, K. Yoshioka-Kobayashi, A. Isomura, R. Kageyama, ES cell-
448 derived presomitic mesoderm-like tissues for analysis of synchronized oscillations in the
449 segmentation clock. *Development* **145** (2018).

450 26. Y. B. Kiyohara *et al.*, The BMAL1 C terminus regulates the circadian transcription
451 feedback loop. *Proc Natl Acad Sci U S A* **103**, 10074-10079 (2006).

452 27. S. C. van den Brink *et al.*, Single-cell and spatial transcriptomics reveal somitogenesis in
453 gastruloids. *Nature* **582**, 405-409 (2020).

454 28. M. Kanehisa, S. Goto, KEGG: kyoto encyclopedia of genes and genomes. *Nucleic Acids*
455 *Res* **28**, 27-30 (2000).

456 29. Y. Niwa *et al.*, The initiation and propagation of Hes7 oscillation are cooperatively
457 regulated by Fgf and notch signaling in the somite segmentation clock. *Dev Cell* **13**, 298-
458 304 (2007).

459 30. M. Matsuda *et al.*, Recapitulating the human segmentation clock with pluripotent stem
460 cells. *Nature* **580**, 124-129 (2020).

461 31. N. Koike *et al.*, Transcriptional architecture and chromatin landscape of the core circadian
462 clock in mammals. *Science* **338**, 349-354 (2012).

463 32. M. Ebisuya, T. Yamamoto, M. Nakajima, E. Nishida, Ripples from neighbouring
464 transcription. *Nat Cell Biol* **10**, 1106-1113 (2008).

465 33. D. M. Owens, S. M. Keyse, Differential regulation of MAP kinase signalling by dual-
466 specificity protein phosphatases. *Oncogene* **26**, 3203-3213 (2007).

467 34. R. T. Moon, J. D. Brown, J. A. Yang-Snyder, J. R. Miller, Structurally related receptors
468 and antagonists compete for secreted Wnt ligands. *Cell* **88**, 725-728 (1997).

469 35. J. K. Dale *et al.*, Periodic notch inhibition by lunatic fringe underlies the chick
470 segmentation clock. *Nature* **421**, 275-278 (2003).

471 36. Z. Chen *et al.*, Identification of diverse modulators of central and peripheral circadian
472 clocks by high-throughput chemical screening. *Proc Natl Acad Sci U S A* **109**, 101-106
473 (2012).

474 37. Y. Inada *et al.*, Cell and tissue-autonomous development of the circadian clock in mouse
475 embryos. *FEBS Lett* **588**, 459-465 (2014).

476 38. C. A. Schneider, W. S. Rasband, K. W. Eliceiri, NIH Image to ImageJ: 25 years of image
477 analysis. *Nat Methods* **9**, 671-675 (2012).

478 39. H. M. T. Choi *et al.*, Third-generation in situ hybridization chain reaction: multiplexed,
479 quantitative, sensitive, versatile, robust. *Development* **145** (2018).

480 40. A. M. Bolger, M. Lohse, B. Usadel, Trimmomatic: a flexible trimmer for Illumina
481 sequence data. *Bioinformatics* **30**, 2114-2120 (2014).

482 41. N. R. Coordinators, Database resources of the National Center for Biotechnology
483 Information. *Nucleic Acids Res* **46**, D8-D13 (2018).

484 42. A. Dobin *et al.*, STAR: ultrafast universal RNA-seq aligner. *Bioinformatics* **29**, 15-21
485 (2013).

486 43. H. Li *et al.*, The Sequence Alignment/Map format and SAMtools. *Bioinformatics* **25**, 2078-
487 2079 (2009).

488 44. A. Frankish *et al.*, GENCODE reference annotation for the human and mouse genomes.
489 *Nucleic Acids Res* **47**, D766-D773 (2019).

490 45. S. Heinz *et al.*, Simple combinations of lineage-determining transcription factors prime
491 cis-regulatory elements required for macrophage and B cell identities. *Mol Cell* **38**, 576-
492 589 (2010).

493 46. M. I. Love, W. Huber, S. Anders, Moderated estimation of fold change and dispersion for
494 RNA-seq data with DESeq2. *Genome Biol.* **15**, 550 (2014).

495 47. Y. Liao, J. Wang, E. J. Jaehnig, Z. Shi, B. Zhang, WebGestalt 2019: gene set analysis
496 toolkit with revamped UIs and APIs. *Nucleic Acids Res* **47**, W199-W205 (2019).

497 48. H. Yoshitane *et al.*, Roles of CLOCK phosphorylation in suppression of E-box-dependent
498 transcription. *Mol Cell Biol* **29**, 3675-3686 (2009).

499

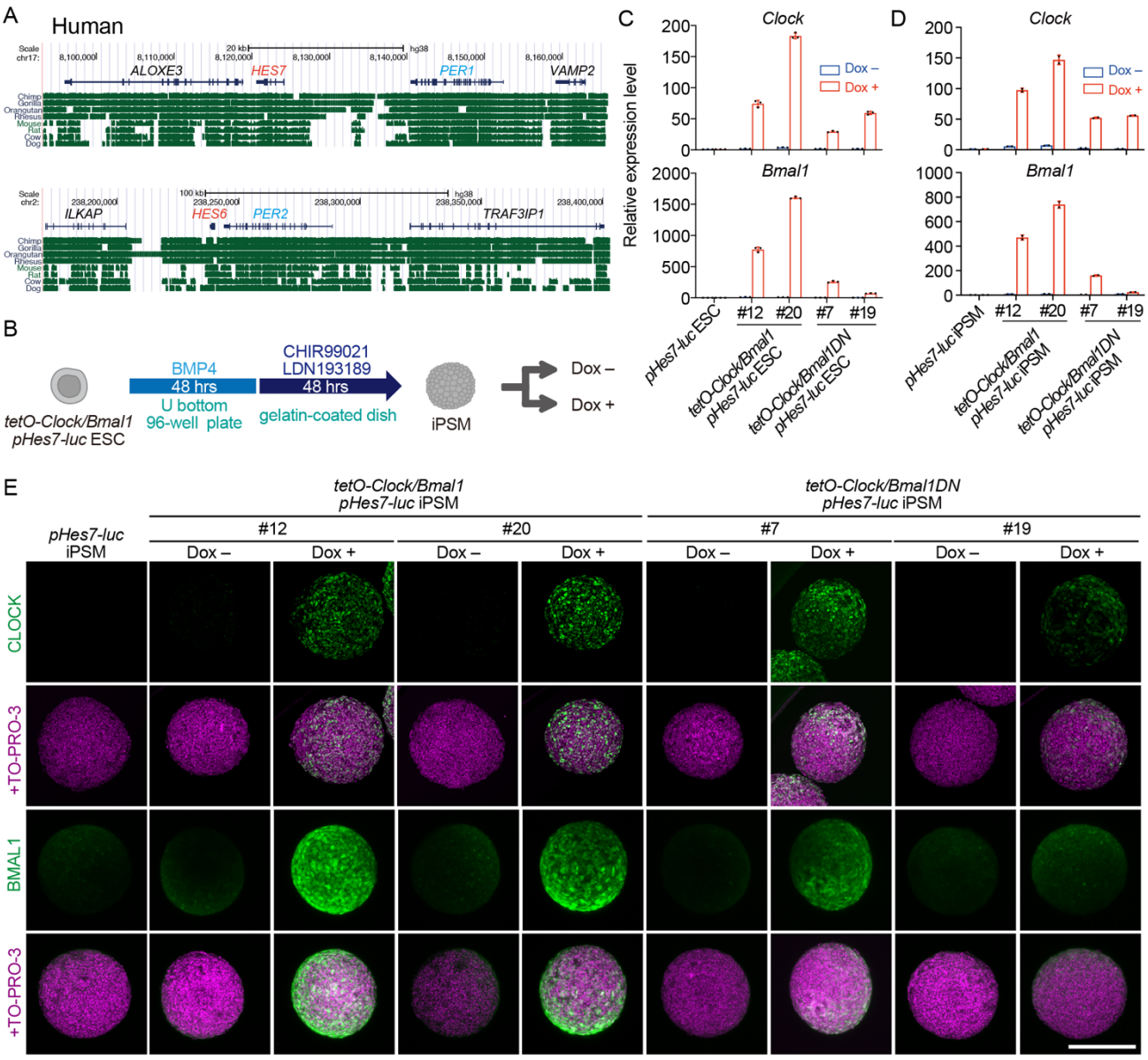

Fig. 1. Establishment of ESC lines carrying both the dox-inducible *Clock* and *Bmal1* genes. (**A**) Human genomic locus of circadian clock genes, *PER1*, and the essential segmentation clock gene, *HES7*, are highly conserved in higher vertebrates. The *PER1* homolog *PER2* is also located adjacent to the *HES7* homolog *HES6* in the genome. (**B**) ESCs were differentiated into iPSM for 96 hr *in vitro*, and then the iPSM colonies were treated with or without dox. (**C**) qPCR of *Clock* and *Bmal1* mRNA in the indicated ESCs. 500 ng/mL dox treatment for 6 hr (red) or not (blue). Each number indicates clone number. Mean ± SD (n = 3 biological replicates). (**D**) qPCR of *Clock* and *Bmal1* mRNA in the indicated iPSM colonies. 1000 ng/mL dox treatment for 2 hr (red) or not (blue). Mean ± SD (n = 2 technical replicates). The average expression level of *pHes7-luc* ESCs or iPSM colonies without dox was set to 1. (**E**) Representative maximum intensity projection of

510 the immunostaining of iPSM colonies treated with 1000 ng/mL dox for 2 hr or not. n = 2–3
511 biological replicates. Scale = 250 μm.

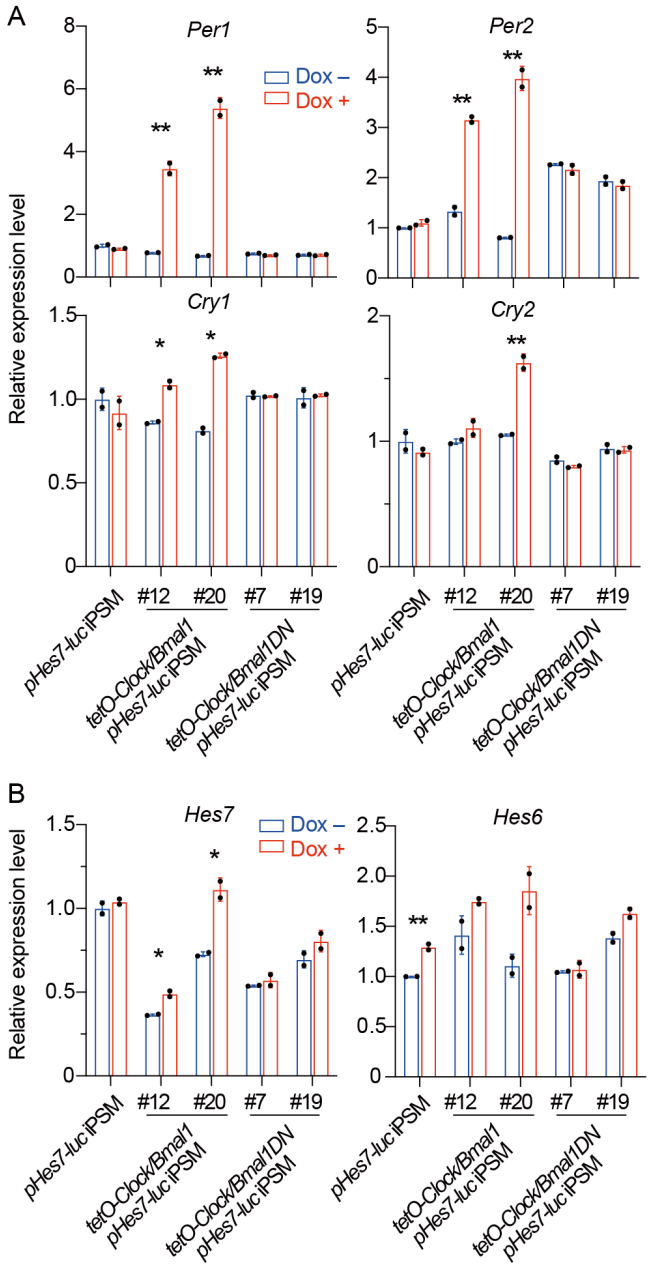

512 **Fig. 2. CLOCK/BMAL1 expressions upregulated not only circadian clock genes but also**
513 ***Hes7* gene expressions in the iPSM.** (**A, B**) qPCR of core circadian clock genes (**A**) and *Hes*7 or
514 *Hes6* gene (**B**) in the indicated iPSM colonies. 1000 ng/mL dox treatment for 2 hr (red) or not
515 (blue). Mean ± SD (n = 2 technical replicates). The average expression level of iPSM colonies
516 without dox was set to 1. Two-tailed t-test, *P < 0.05, **P < 0.01.

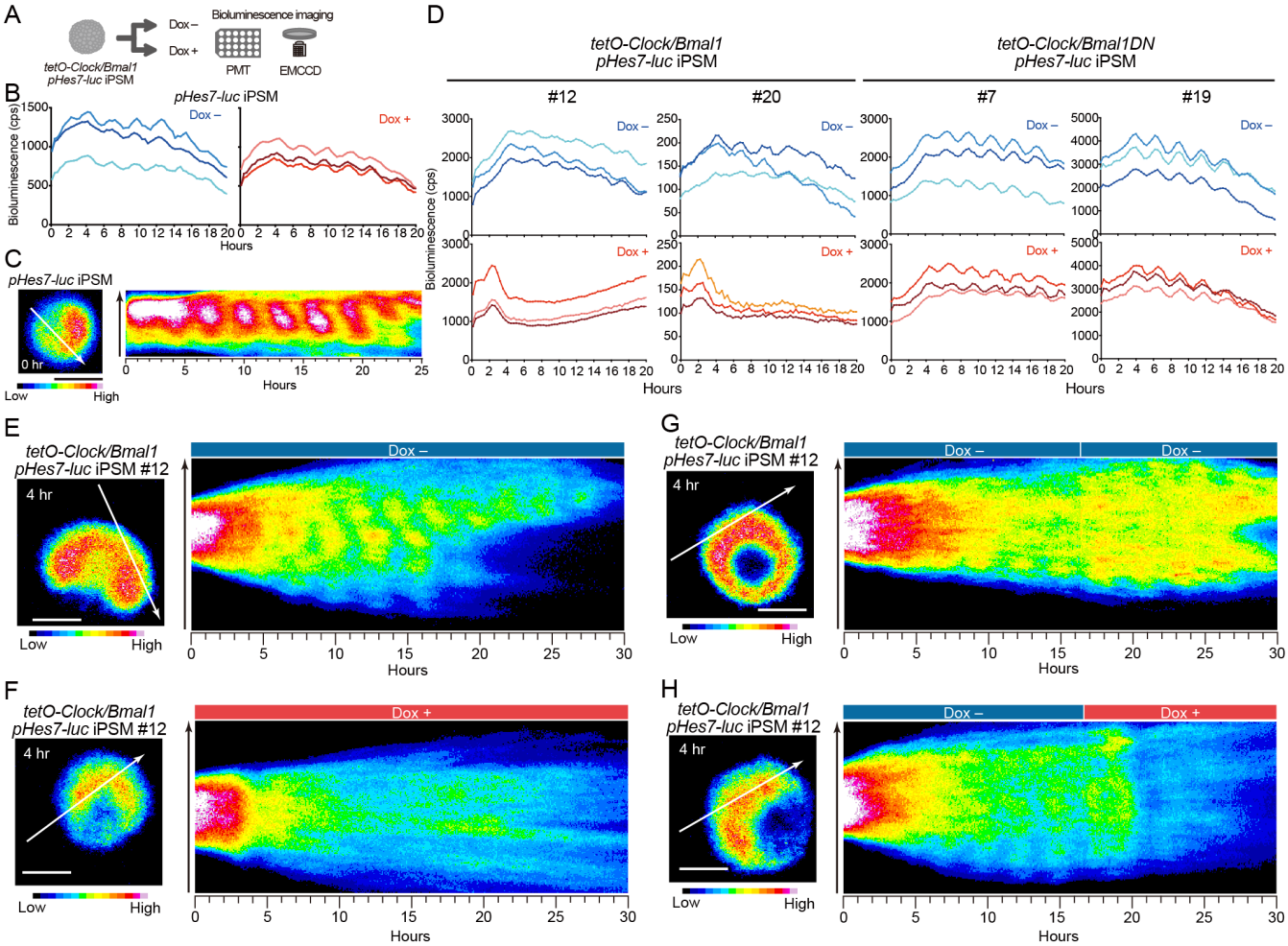

Fig. 3. CLOCK/BMAL1 expressions arrested the autonomous oscillations of *Hes7* in the iPSM colonies. (**A**) Bioluminescence of each dox-inducible *Clock/Bmal1* or *Clock/Bmal1DN pHes7-luc* iPSM colony was observed using PMT or an EM-CCD camera without or with dox. (**B, C**) Representative bioluminescence traces (**B**, n = 25 biological replicates) and live imaging (**C**, n = 3 biological replicates) of single *pHes7-luc* iPSM colony with or without dox. The kymograph of the imaging along the arrow is shown. (**D**) Representative bioluminescence traces of the single indicated iPSM colony with and without 1000 ng/mL dox. n = 10-54 biological replicates. (**E–H**) Live imaging of the single *tetO-Clock/Bmal1 pHes7-luc* iPSM colony with and without dox. Dox-containing medium or only medium was added at the indicated time points at the final dox concentration of 1000 ng/mL (**G, H**). Each kymograph along the arrow is shown. Scales = 250 µm. n = 2-4 biological replicates.

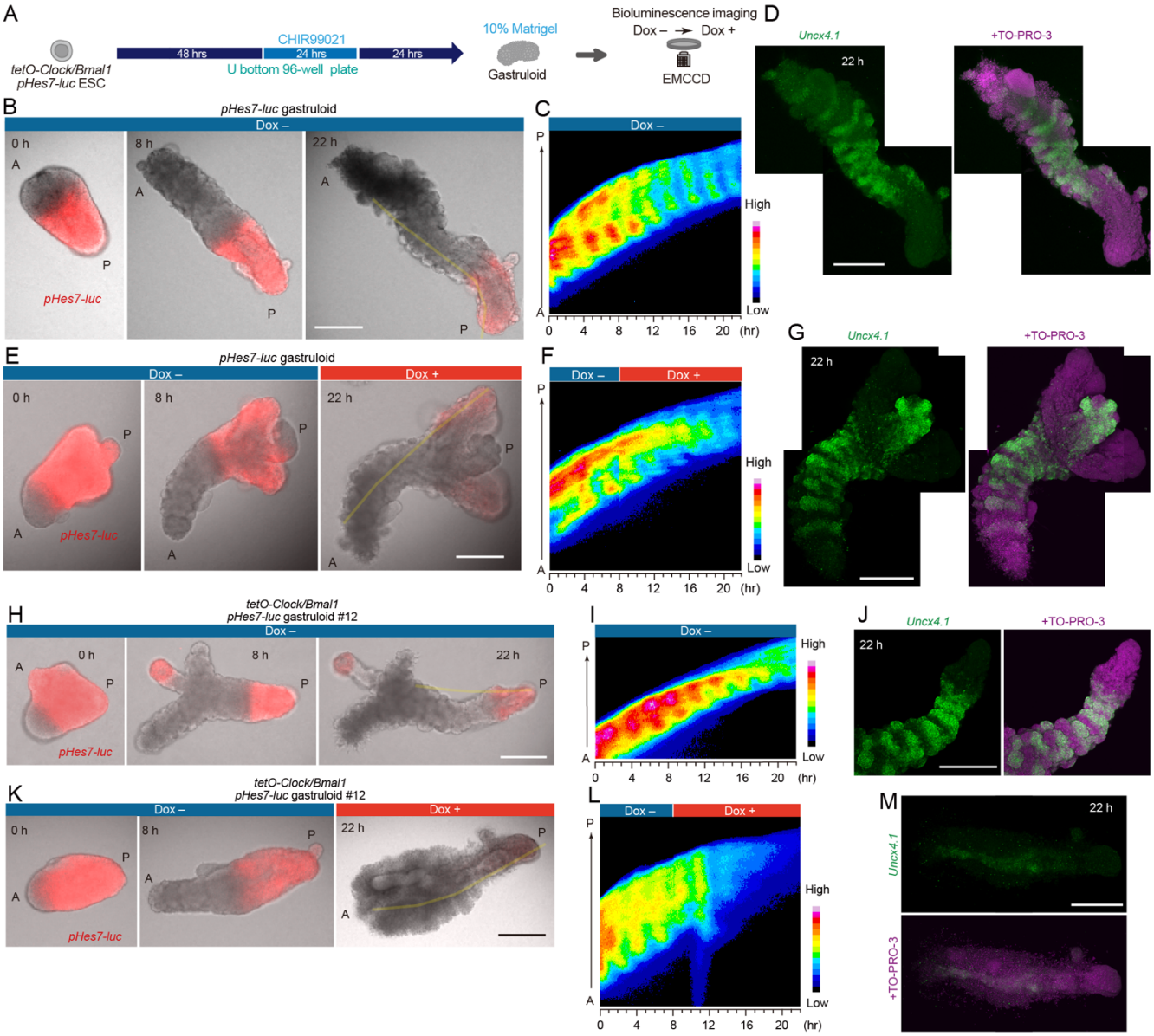

528 **Fig. 4. CLOCK/BMAL1 expressions interfered with the autonomous oscillations of *Hes7* and**
529 **somitogenesis-like process in the gastruloids.** (**A**) Dox-inducible *Clock/Bmal1 pHes7-luc* ESCs
530 were differentiated into gastruloids for 96 hr *in vitro*, and then the gastruloids embedded in 10%
531 Matrigel were treated with or without dox. *pHes7-luc* bioluminescence was observed using an EM-
532 CCD camera without or with dox. (**B–M**) Time-lapse bioluminescence (red) and bright field
533 imaging of the single *pHes7-luc* gastruloid or *tetO-Clock/Bmal1 pHes7-luc* gastruloid without and
534 with dox. Dox-containing medium was added at the indicated time points at the final dox
535 concentration of 1000 ng/mL (**C, F, I, L**). Each kymograph is shown along the yellow lines in **B,**
536 **E, H, K**. *In situ* hybridization of *Uncx4.1* in the gastruloids after the live cell imaging (**D, G, J,**
537 **M**). Scales = 250 µm. n = 2-4 biological replicates.

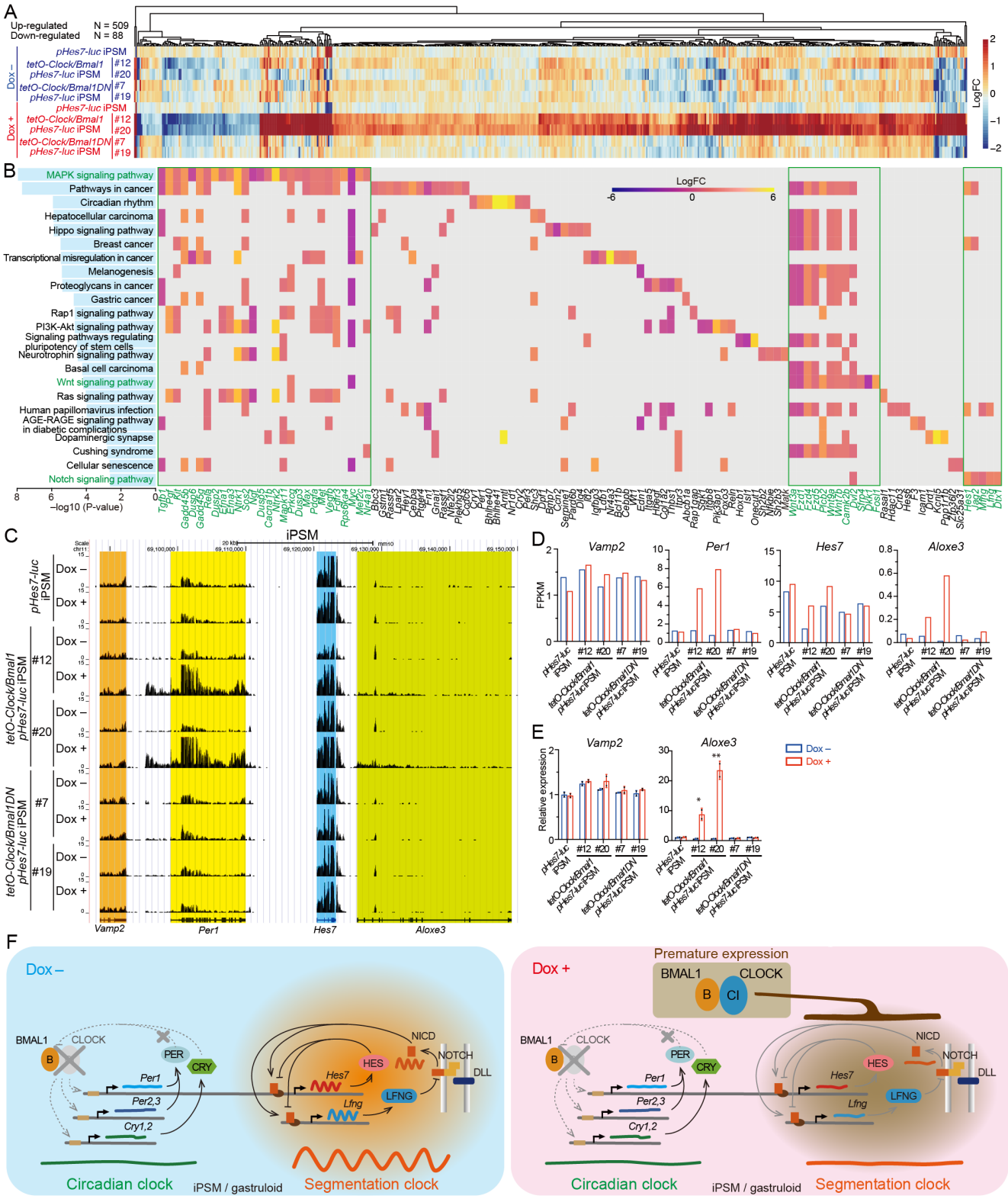

Fig. 5. CLOCK/BMAL1 expressions in the iPSM colonies affected *Hes7*-related signaling pathways and upregulated the expression of contiguous genes, *Per1*, *Hes7*, and *Aloxe3*. (**A**) Upregulated and downregulated DEGs in the indicated iPSM colonies treated with dox. (**B**) KEGG

541 pathway analysis of the DEGs. Each pathway was indicated with each transformed p-value. The
542 ranked pathways contained several common genes in the WNT, MAPK, and NOTCH signaling
543 pathways. (**C**) UCSC genome browser views of RNA-seq data of the contiguous genes *Vamp2*,
544 *Per1*, *Hes7*, and *Aloxe3*. The reads shown are normalized average reads per 10 million total reads
545 in 10-bp bins. (**D**) mRNA expression of *Vamp2*, *Per1*, *Hes7*, and *Aloxe3* in the indicated iPSM
546 colonies according to RNA-seq. (**E**) Validation of *Vamp2* and *Aloxe3* gene expression levels in
547 the indicated iPSM colonies using qPCR. Colored boxes indicate 1000 ng/mL dox treatment for 2
548 hr (red) or no treatment (blue). Mean ± SD (n = 2 technical replicates). The averaged expression
549 level of *pHes7-luc* iPSM colonies without dox was set to 1. Two-tailed t-test, *P < 0.05, **P <
550 0.01. (**F**) The premature expression of CLOCK/BMAL1 in the iPSM and gastruloids interfered
551 with the segmentation clock oscillation and somitogenesis-like process.

Supporting information for

Circadian key component CLOCK/BMAL1 interferes with segmentation clock in mouse embryonic organoids

Yasuhiro Umemura, Nobuya Koike, Yoshiki Tsuchiya, Hitomi Watanabe, Gen Kondoh, Ryoichiro Kageyama, and Kazuhiro Yagita

Correspondence to: kyagita@koto.kpu-m.ac.jp

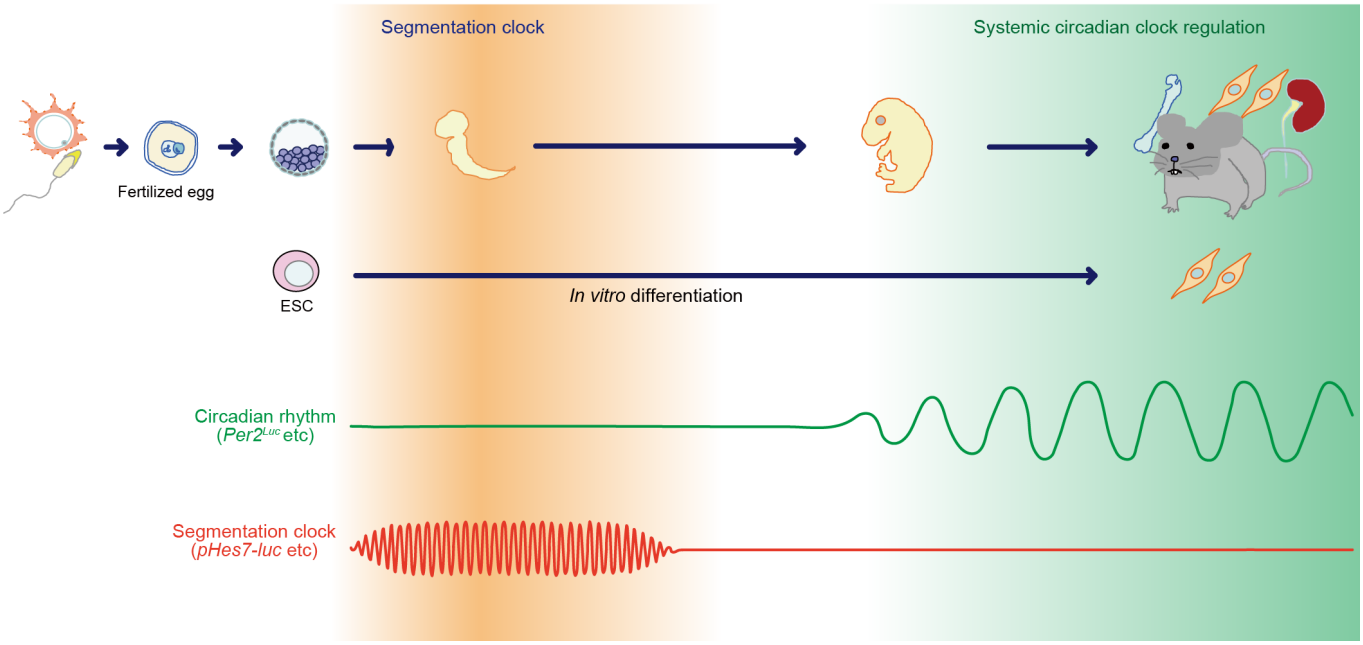

Fig. S1. Mutually exclusive appearance of segmentation clock and circadian clock. In mammals, two different types of rhythm appear sequentially during the developmental process. One is the ultradian rhythm by segmentation clock, which controls somitogenesis. The other one is the circadian oscillation, which regulates the predictive adaptation of physiological functions to the day–night environmental cycle.

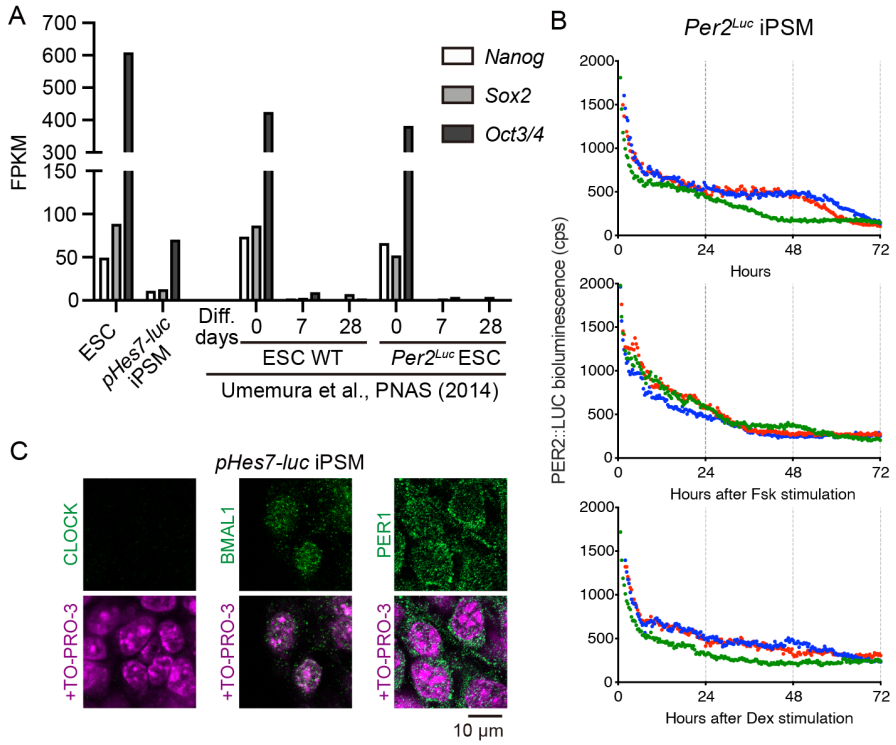

Fig. S2. The iPSM has no apparent circadian clock oscillation. (A) The expression levels of pluripotent marker genes, *Nanog*, *Sox2*, and *Oct3/4,* were measured using RNA-seq in ESCs and *pHes7-luc* iPSM. The data were shown with *in vitro* 0, 7-, and 28-day differentiated WT ESCs and *Per2*^{Luc} ESCs (GSE61184). No circadian clock oscillates in the *in vitro* 7-day differentiated ESCs and the circadian clock oscillation starts to emerge after 14 days of differentiation culture (16, 17). **(B)** Bioluminescence traces of the iPSM differentiated from *Per2*^{Luc} ESCs. The iPSM was stimulated with 10 μM forskolin (Fsk, middle) or 100 nM dexamethasone (Dex, bottom). n = 3 biological replicates. **(C)** Representative immunostaining of CLOCK, BMAL1, and PER1 in the iPSM. The immunostaining represented the suppression of CLOCK proteins in contrast to the expression of BMAL1. Furthermore, although the nuclei indicated the quite faint signals, PER1 protein in the iPSM is still predominantly accumulated in the cytoplasm.

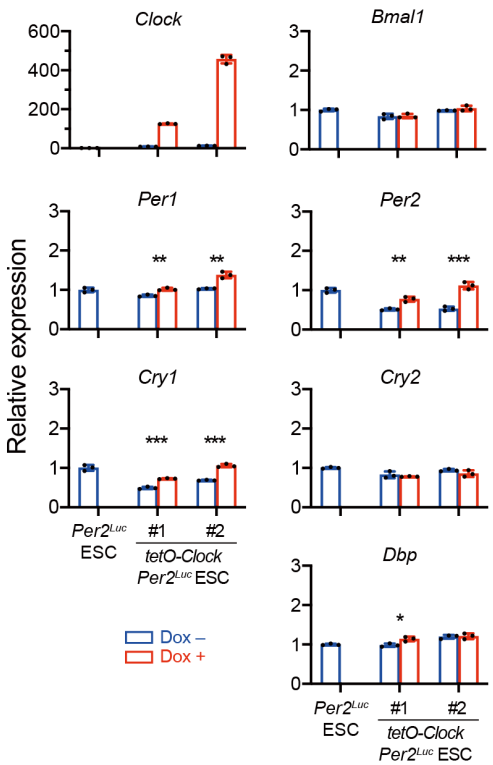

Fig. S3. The core circadian clock gene expressions in the ESCs harboring dox-inducible *Clock*. Although the expression of BMAL1 protein was observed even in ESCs (17), dox-dependent sole expression of *Clock* was insufficient for the E-box-driven expression of clock genes such as *Per1/2* and *Cry1/2* in undifferentiated ESCs, raising the possibility that the endogenously expressed BMAL1 might be post-translationally modified to not function. Colored boxes indicate 500 ng/mL dox treatment for 6 hr (red) or no treatment (blue). Each number indicates clone number. Mean ± SD (n = 3 biological replicates). The averaged expression level of *Per2*^{Luc} ESCs without dox was set to 1. Two-tailed t-test, *P < 0.05, **P < 0.01, ***P < 0.001.

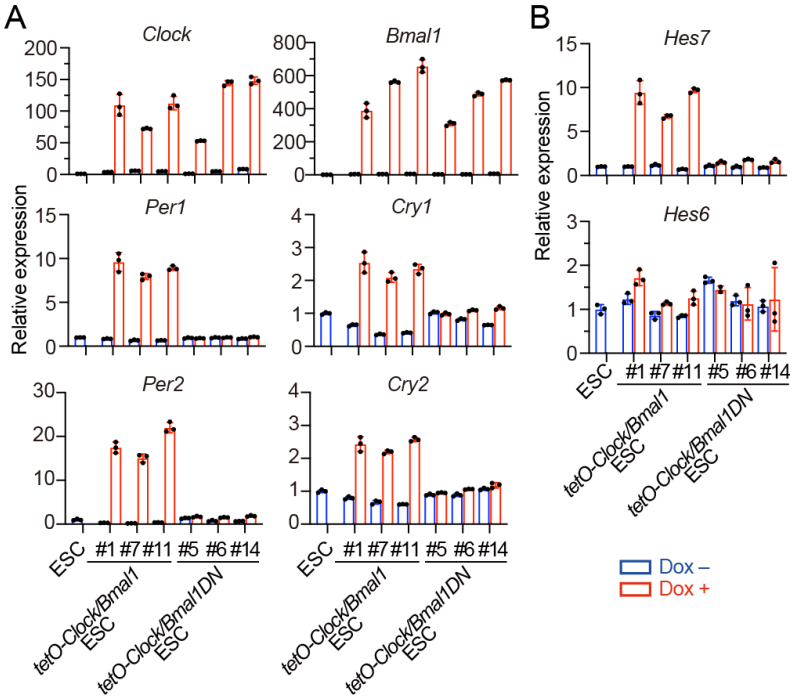

Fig. S4. *Clock/Bmal1* gene expressions in ESCs upregulated not only circadian clock genes but also *Hes7* gene expression. (**A, B**) qPCR of core circadian clock gene (**A**) and *Hes*7 or *Hes6* gene (**B**) expression in ESCs harboring dox-inducible *Clock* and *Bmal1* or *Clock* and *Bmal1DN*. Colored boxes indicate the presence (red) or absence (blue) of 500 ng/mL dox treatment for 6 hr. Each number indicates clone number. Mean ± SD (n = 2–3 biological replicates). The average expression level of ESCs without dox was set to 1.

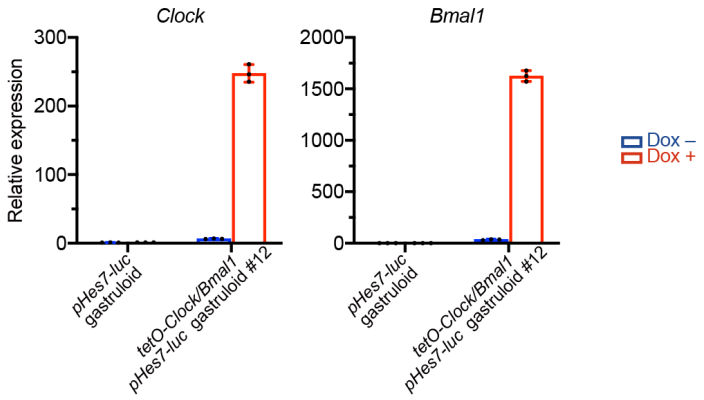

Fig. S5. qPCR of *Clock* and *Bmal1* mRNA in the indicated gastruloids. Colored boxes indicate 1000 ng/mL dox treatment for 2 hr (red) or no treatment (blue). Each number indicates clone number. Mean ± SD (n = 3 biological replicates). The average expression level of *pHes7-luc* gastruloids without dox was set to 1.

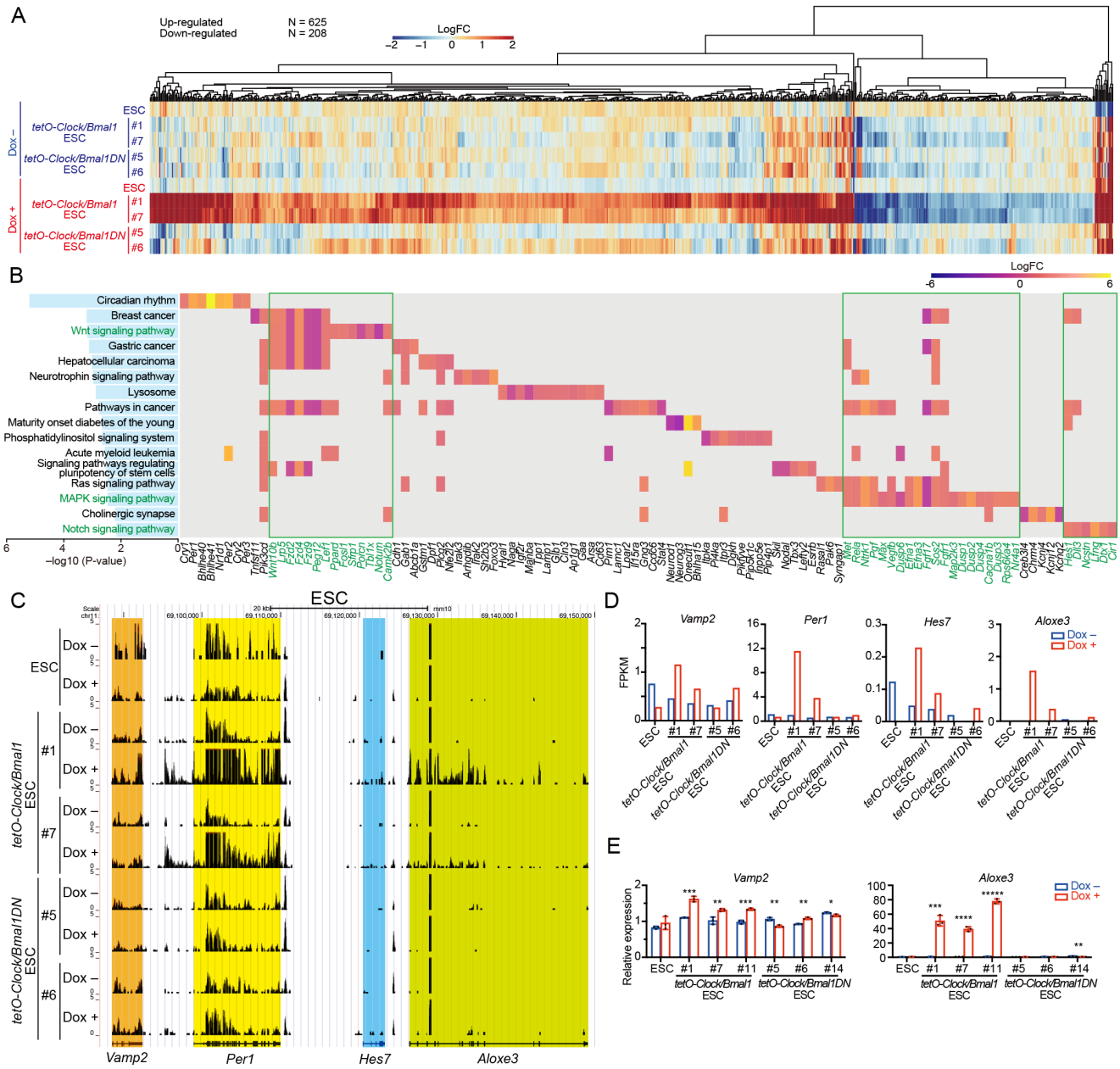

Fig. S6. *Clock/Bmal1* gene expressions in ESCs affected the *Hes7*-related signaling pathways and upregulated the expression of the contiguous genes *Vamp2, Per1*, *Hes7*, and *Aloxe3*. (**A**) Upregulated and downregulated differentially expressed genes in the indicated ESCs treated with dox (FDR < 0.05, FC > 1.5). (**B**) KEGG pathway analysis of the DEGs. Each pathway was indicated with each transformed p-value. The ranked pathways contained several common genes in the WNT, MAPK, and NOTCH signaling pathways. (**C**) UCSC genome browser views of RNA-seq data of contiguous genes, including *Vamp2*, *Per1*, *Hes7*, and *Aloxe3*. The reads shown are normalized average reads per 10 million total reads in 10-bp bins. (**D**) mRNA expression of *Vamp2*, *Per1*, *Hes7*, and *Aloxe3* in the indicated ESCs measured using RNA-seq. (**E**) Validation of *Vamp2*

52 and *Aloxe3* in the indicated ESCs by qPCR. Colored boxes indicate the use of 500 ng/mL dox
53 treatment for 6 hr (red) or untreated cells (blue). Each number indicates clone number. Mean ± SD
54 (n = 3 biological replicates). Two-tailed t-test, *P < 0.05, **P < 0.01, ***P < 0.001, ****P <
55 0.0001, *****P < 0.00001.